Earth and Planetary Science Letters, 118 (1993) 295–309
Elsevier Science Publishers B.V., Amsterdam

[MK]

Uplift and thermal history of the Teton Range (northwestern Wyoming) defined by apatite fission-track dating

Susan V. Roberts [1] and Douglas W. Burbank

Department of Geological Sciences, University of Southern California, Los Angeles, CA 90089, USA

Received November 25, 1992; revision accepted May 18, 1993

ABSTRACT

In order to determine the pattern and timing of exhumation and uplift in the Teton Range, fission-track analysis of apatites has been applied to three sections encompassing ~2 km of vertical relief along the Teton escarpment. The resulting data provide new insights on the doming of the Precambrian–Cambrian unconformity and on the Teton exhumation/uplift history prior to the Miocene initiation of range-front faulting.

Each section exhibits successively younger fission-track ages with decreasing sample elevation. The majority of these dates are between 85 and 65 my. Mean track lengths decrease and the statistical distribution of track lengths broadens with decreasing elevation. These data indicate Late Cretaceous cooling and an inferred uplift of 1–2 km. Younger dates (26–67 my) and typically broader track-length histograms characterize the northernmost section. Although mid-to-late Cenozoic volcanic heat sources could have perturbed the northern section, modeling of two reasonable thermal sources indicates that such heat perturbation is unlikely. Instead, it appears that this section and the lower parts of the more southerly sections, which also exhibit broad track-length distributions, resided in the partial annealing zone for a considerable span of the Tertiary.

The Laramide deformation in the Tetons involved both uplift and folding of the basement, rather than being restricted to compressional structures within the Phanerozoic strata. Consequently, deep-seated, basement-involved structures must have been active beneath the range in the Late Cretaceous. The fission-track data suggest that the most extensive, post-Cretaceous uplift occurred in the northern part of the Teton Range and resulted in a southward tilt of 2–3° between the northernmost and southernmost sections. To the extent discernable from the fission-track data, much of the arching of the Precambrian–Cambrian unconformity occurred in the Late Cretaceous and was rotated into its present position by differential footwall uplift during late Cenozoic extension.

1. Introduction

Fission-track analysis applied to uplifted areas can provide data concerning the rates, timing, and history of cooling, exhumation, and uplift in a relatively rapid and reliable manner [1–3]. When combined with geologically calibrated rates and ages of uplift, fission-track data can yield insights on the thermal and topographic evolution of a region.

An exceptional area for such a combined study is the Teton Range in northwestern Wyoming (Fig. 1). This block of approximately 2 billion year old Precambrian gneiss and granite [4], uplifted by Late Tertiary extensional normal faulting [5], was only modestly deformed by Laramide and Tertiary compression. The topographic emergence of the present range began around 9 Ma [6] and exposed Precambrian rocks which are > 4 km above sea level today. At the largest scale, the range dips as a block toward the west, but doming of the Precambrian–Cambrian unconformity at the top of the range also indicates a distinctive uplift style in which the convexity of the unconformity resulted from differential uplift of the center of the range ~2 km higher than the northern and southern ends.

Criteria for using fission-track analysis in an uplift study include the presence of appropriate minerals and an estimate of burial depths [1–

[1] Present address: Engineering-Science, Inc., 7800 Shoal Creek Rd. #222 West, Austin, TX 78757, USA.

0012-821X/93/$06.00

3,7,8]. Teton gneisses and granites contain apatite which is suitable for fission-track analysis. The stratigraphy of Teton Range and associated basins suggests that 2–4 km of pre-Tertiary strata could have buried the range before Miocene faulting [9]. Geophysical study of the Teton region [10] shows basement at 5 km below the surface of Jackson Hole (Fig. 2). Because the highest peaks in the Teton Range also comprise basement rocks and rise ~ 2 km above the valley floor, there is a vertical basement offset of 7 km [10] that is interpreted to have developed during the last 9 my [9].

Fission-track data in this study, as interpreted in terms of timing of exhumation, rates and style of uplift, and thermal history of uplift, are compared to uplift information taken from the vertical offset across the range of two Plio-Pleistocene-aged tuffs and the post-Miocene stratigraphic evidence for a rising Teton Range [6,9]. This comparison sheds light both on the history of Teton uplift and on the utility and limitations of apatite fission-track analysis.

2. Regional geology

Laramide structures, Cenozoic volcanic terranes, and Neogene extensional structures dominate the present geology of northwestern Wyoming and southwestern Montana (Fig. 1). Major Laramide-aged, basement-cored uplifts of this Late Cretaceous to early Eocene orogenesis include the Wind River Range and the Beartooth Mountains. The Eocene-aged Absaroka volcanic field forms a highland to the northeast of Jackson Hole. The Plio-Pleistocene Yellowstone rhyolitic plateau and the Late Tertiary Snake River downwarp delineate the northern and southwestern margins of the Teton uplift, whereas the extensional basin of Jackson Hole defines the eastern boundary of the uplift (Figs. 1 and 2).

Throughout most of the Mesozoic era, the Precambrian core of the Tetons was buried beneath ~ 1.5 km of Paleozoic strata as defined by stratigraphy on the north and west flanks of the range [9]. An additional 2–3 km of Mesozoic strata are likely to have covered the range prior to the beginning of Laramide deformation. The thick, coarse-grained conglomerates of the Upper Cretaceous Harebell Formation and Paleocene Pinyon Conglomerate presently preserved in Jackson Hole [9] are unlikely to have blanketed the range extensively, given the syntectonic exhumation that is demonstrated by the present study. The distribution of these gold-bearing, quartzitic conglomerates is interpreted to have resulted from Laramide deformation in the Teton area [6,11]. Whereas paleocurrent directions and the clast lithologies are compatible with a potential source area in the buried Targhee uplift [6], located northwest of an assumed low-lying Teton Range, it appears more likely that the quartzite was supplied to the Harebell and Pinyon conglomerates by passive hanging-wall uplift over hinterland ramps of regional thrust systems [11].

In the Teton Range–Jackson Hole area, Laramide deformation is also indicated by thrust-related shortening within the southern Teton Range [12] and across much of the Gros Ventre Range. Several Laramide-aged thrust faults have been identified in the southern Teton Range [12], including the Buck Mountain, Stewart, and Static faults. The magnitude of displace-

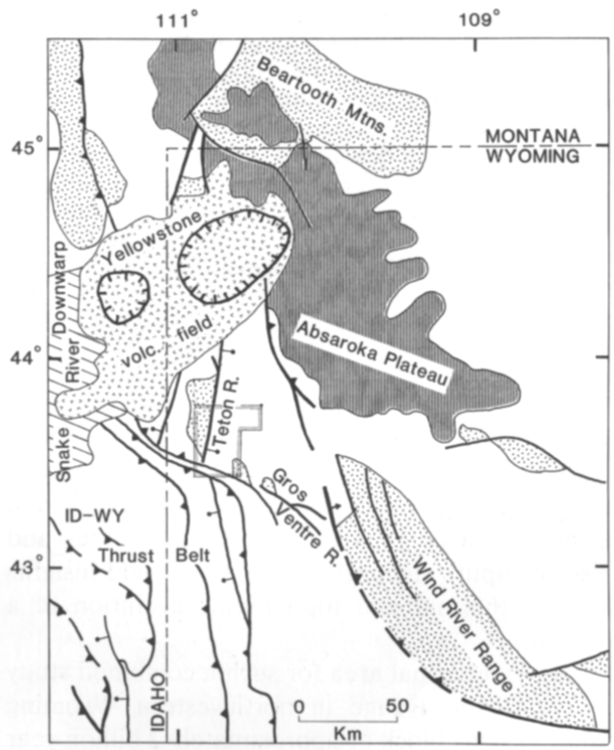

Fig. 1. Simplified geologic map of northwest Wyoming, southwest Montana, and eastern Idaho, after Love [9]. Hatched pattern indicates Precambrian-cored ranges; random V pattern is the Yellowstone volcanic field, with the major calderas outlined. Area within shaded box is the location of Fig. 2.

ment along these faults is poorly known, but reconstructions for the Buck Mountain Fault [12] suggest that it may have accommodated as much as 1 km of shortening and may have soled into the deeper seated Cache Creek thrust. The surface trace of the Cache Creek fault runs perpendicular to the Teton normal fault and appears to delineate its southernmost expression (Fig. 2).

Subsidence in the northern part of Jackson Hole in the mid-Tertiary is indicated by the early and middle Miocene-aged Colter Formation, a thick volcanic and volcaniclastic succession [13]. The Teewinot Formation, comprising lacustrine and tuffaceous strata > 1 km thick, accumulated in central and southern Jackson Hole during the late Miocene. The absence of coarse detritus in the Teewinot Formation has been interpreted to indicate that the Tetons probably had not risen to any great height by 9–10 Ma [6].

Late Cenozoic hanging-wall subsidence of the Precambrian basement to ~ 5 km beneath the present surface of Jackson Hole and coeval footwall uplift and westerly tilt of the Teton Range to ~ 2 km above the present surface are indicated by geophysical and stratigraphic data [9,10]. The 4 Ma Conant Creek Tuff and the 2.05 Ma Huckleberry Ridge Tuff are preserved in both the hanging wall and footwall of the Teton normal fault. Structural offsets of these tuffs indicate a minimum of 1520 and 1220 m of vertical separation, respectively, since they were erupted [6].

3. Methodology

In the Teton area, apatite and zircon occur in the Precambrian granites and gneisses and in Phanerozoic sandstones, where they occur as detrital minerals. Three sections, spaced 12–17 km

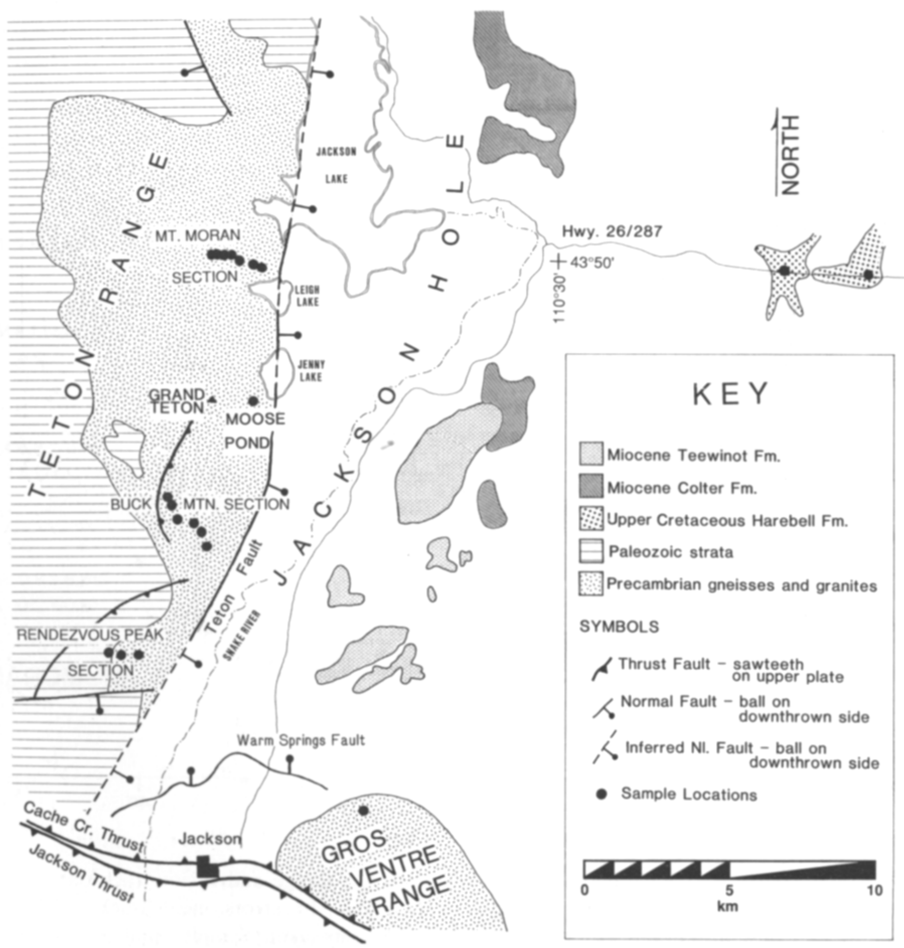

Fig. 2. Simplified geologic map of the Teton Range, selected elements of Jackson Hole, and the northern end of the Gros Ventre Range. Major faults, locations of fission-track sampling sites, and the line of cross-sections in subsequent figures are depicted.

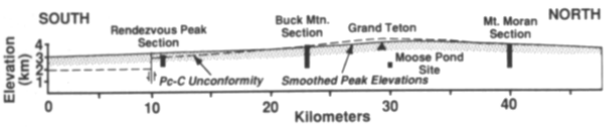

Fig. 3. Longitudinal section approximately along the smoothed crest of the Teton Range, on to which are projected the altitudinal range (bars) encompassed by fission-track sites at each section. Peak elevations depicted by smooth line and Precambrian–Cambrian unconformity by dashed line. No vertical exaggeration.

apart and oriented perpendicular to the range front, were sampled along the eastern escarpment of the Teton Range (Figs. 2 and 3): the Rendezvous Peak section in the south, the south-central Buck Mountain section, and the Mount Moran section in the north. To the extent permitted by available exposures along these topographically inclined traverses, samples were collected in vertical intervals of ~ 300 m. Additional samples were collected from low-elevation sites in the Teton and Gros Ventre Ranges and from the Harebell Formation (Fig. 2).

Refinement of the cooling and uplift history of the Teton Range was undertaken in this study through an analysis of the fission-track dates of individual apatite grains and of the distributions of fission-track lengths within each sample. Fis-

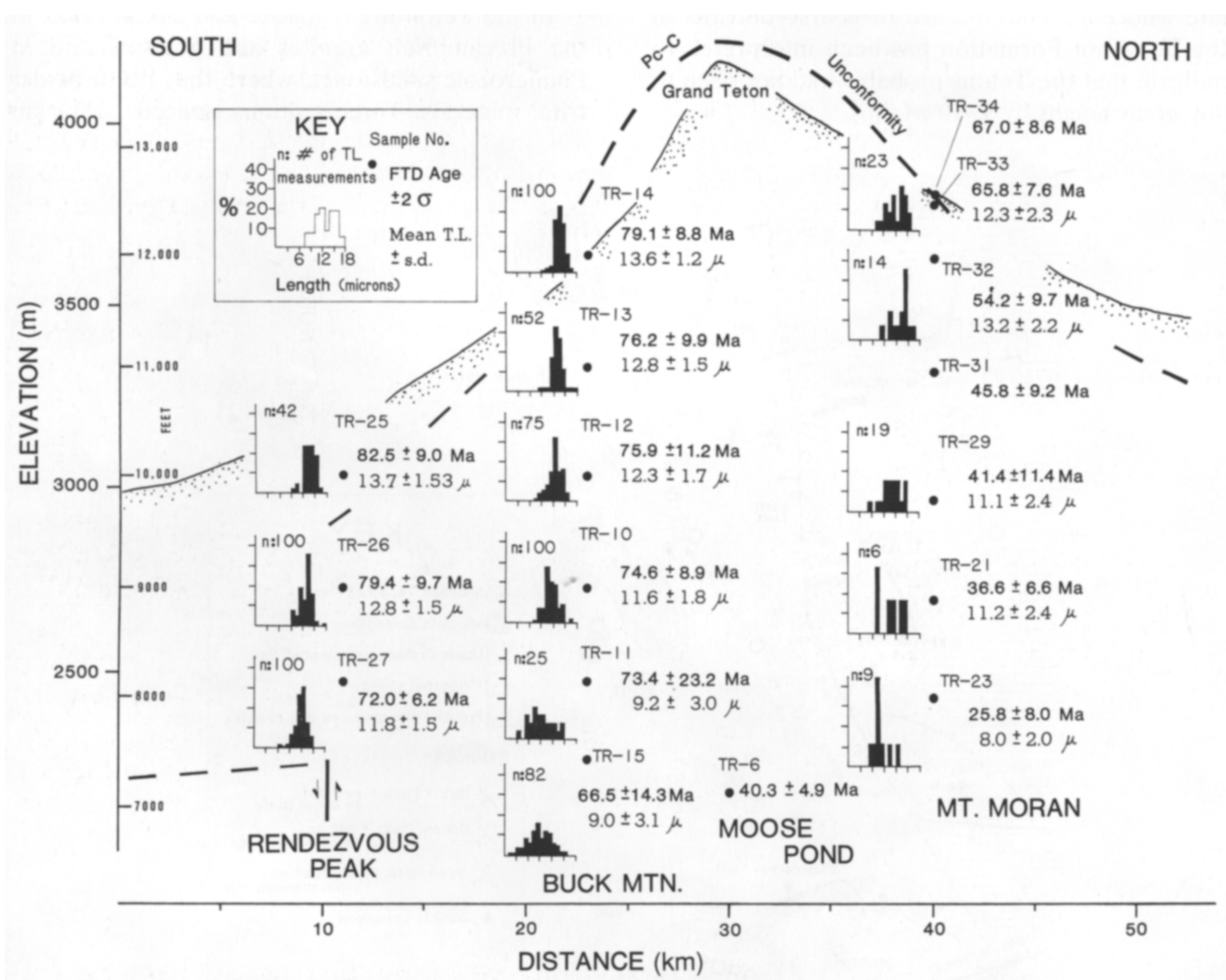

Fig. 4. Vertically exaggerated (×18) N–S longitudinal section of the Teton Range and fission-track data corresponding to the sections shown in Figs. 2 and 3. Shown in detail: apatite fission-track ages $\pm 1\sigma$ errors, mean track-length measurements with standard deviations, and track-length histograms with number of measurements taken. Sample number and location are at sample elevations, shown by •. The shaded line is the smoothed N–S profile of the Teton peaks; the dashed line is the Precambrian–Cambrian unconformity. Three samples were not measured for track lengths: TR-34, TR-31, and TR-6.

sion-track dates were calculated using the external detector method [14], which appears to be statistically valid for the Teton apatites, given the relative paucity of defects and the density of fission tracks. Sample collection, processing, and dating was completed between 1986 and 1988.

In accordance with the techniques of Naeser [14] and Gleadow [15], the apatites were mounted in epoxy, polished, etched, overlain with mica, and irradiated by TRIGA reactors to induce ^{235}U fissioning. Six or more apatite/mica pairs were counted for each age calculation, and a 2σ error was calculated for each fission-track age following the statistical method of McGee et al. [16]. In addition, standards of 31 Ma Durango apatite were counted to verify the calibration of the neutron dose. Because apatite has a closure temperature of 100–110°C for track retention over geologically long intervals (> 5 my) [17], the calculated apatite fission-track dates were initially interpreted to record time since the last thermal event of temperatures greater than ~ 105°C for

TABLE 1

Fission-track data for all samples

SAMPLE LOCATION	SAMPLE I.D.	ELEVATION [meters]	NUMBER APATITES COUNTED	FLUENCE x 10^{15} [n/cm^2]	(s) TRACKS COUNTED	(i) TRACKS COUNTED	AGE [Ma]	2-SIGMA ERROR [Ma]
RENDEZVOUS PEAK	TR-25	3030	10	9.89	430	1532	82.5	9.0
	TR-26	2727	9	9.41	341	1202	79.4	9.7
	TR-27	2485	10	9.35	670	2588	72.0	6.2
BUCK MOUNTAIN	TR-14	3636	6	9.71	409	1493	79.1	8.8
	TR-13	3333	11	9.66	302	1139	76.2	9.9
	TR-12	3030	6	9.88	227	879	75.9	11.2
	TR-10	2727	9	10.00	350	1395	74.6	8.9
	TR-11	2485	6	9.94	51	206	73.4	23.2
	TR-15	2242	7	9.65	106	458	66.5	14.3
MOUNT MORAN	TR-34	3818	9	9.63	303	1296	67.0	8.6
	TR-33	3788	9	9.68	371	1625	65.8	7.6
	TR-32	3636	9	9.76	147	788	54.2	9.7
	TR-31	3333	7	9.81	115	735	45.8	9.2
	TR-29	2970	8	9.85	60	426	41.4	11.4
	TR-21	2697	14	9.53	137	1064	36.6	6.6
	TR-23	2424	10	9.47	45	494	25.8	8.0
MOOSE POND	TR-06	2182	12	9.73	302	2169	40.3	4.9
GROS VENTRE	GV-16	2182	8	9.58	333	1323	71.9	8.9
HAREBELL FORMATION	HF-2(up)	2727	10	9.87	468	1880	73.1	7.5
	HF-1(lo)	2485	6	9.94	346	1310	78.1	9.5
DURANGO APATITE CALIBRATION SAMPLES	DUR-A	N/A	5	9.82	87	819	32.2	7.4
	DUR-B	N/A	5	9.59	77	712	30.9	7.3
	DUR-C	N/A	8	9.71	93	861	31.9	6.9

FTD age equation:

$$\text{Age} = \ln\left[1 + \frac{N_s}{N_i}\cdot\frac{\lambda_D\cdot \emptyset\cdot\sigma\cdot I}{\lambda_F}\right]\cdot\frac{1}{\lambda_D}$$

Constants used in age calculations

λ_D = decay constant of $U^{238} = 1.55125\times10^{-10}$/yr;

λ_F = decay constant of spontaneous fission $= 7.03\times10^{-17}$/yr;

I = atomic ratio $U^{235}/U^{238} = 7.25\times10^{-3}$;

σ = neutron fission reaction cross-section = 580.2 barns.

Variables used in age calculations

$\emptyset$ = neutron dose (n/cm^2);

N_s = number of spontaneous tracks counted;

N_i = number of induced tracks counted;

Calibration samples = 31 Ma Durango apatites.

more than ~10 my. These interpretations were subsequently modified in accordance with relevant track-length data for each sample, because previous track-length studies [18–20] indicate that specific patterns of length changes are interpretable as a function of the exposure time to annealing temperatures.

For the track-length measurements, apatites were mounted in epoxy, polished, and etched in 7% nitric acid for 60 s. Measurements of track lengths were made only of horizontal, confined tracks. To ensure reproducibility, the sample measured first was measured again at the end of each session. The track-length data were recorded as the number of tracks measured, their average and median lengths, the standard error (1σ), and the number and percentage of tracks within each μm range.

4. Results

4.1 Apatite ages

Three samples, of which the lower two were Precambrian gneiss and the highest was Cambrian Flathead Sandstone, were collected in the Rendezvous Peak section between ~2500 and 3000 m above sea level (Figs. 2–4). Although the Flathead Sandstone is detrital in origin, individual grain ages indicate cooling below the apatite annealing temperature at approximately the same time as the other Rendezvous Peak samples. The fission-track ages ranged from 72.0 ± 6.2 (2σ) Ma at the base to 82.5 ± 9.0 Ma at the top (Table 1 and Fig. 4).

Six kilometers south of the Grand Teton and 12 km north of the Rendezvous Peak section, six samples were collected from the Buck Mountain section (Figs. 2–4). The fission-track ages of the samples, spaced at ~300 m vertical intervals, varied from 66.5 ± 14.3 Ma (2242 m) to an age of 79.9 ± 8.8 Ma at the summit (3636 m).

The Mount Moran section, 17 km north of the Buck Mountain section, was sampled above 2400 m in six vertical intervals of 300 m, and the top two samples were collected at 3788 and 3818 m from adjacent outcrops of Precambrian gneiss and Cambrian Flathead Sandstone (Figs. 2–4). The sample from the lowest elevation yielded a fission-track age 25.8 ± 8.0 Ma, and the next five samples increase in age to the Cambrian sandstone sample dated at 67.0 ± 8.6 Ma. Clear evidence that the fission-track ages indicate cooling ages, rather than geologic ages, is provided by the concordant fission-track ages of the 2 Ga gneiss (65.8 ± 7.6 Ma at 3788 m) and the Cambrian Flathead Sandstone (67.0 ± 8.6 Ma) at the summit. Note that the ages of these topmost samples are close to ages of the lowest samples from the other two sections.

The fission-track ages of the three sections show a clear trend of increasing age with increasing elevation (Fig. 4 and Table 1). Although the 2σ errors indicate overlap among the ages in each section, the overall trend persists.

The Moose Pond low-elevation sample, collected at 2182 m between the Buck Mountain and Mount Moran sections, yielded a fission-track age of 40.3 ± 4.9 Ma (Figs. 2–4). A 2182 m elevation sample collected about 700 m below the Precambrian–Cambrian unconformity in the Gros Ventre Range yielded a fission-track age of 71.9 ± 8.9 Ma (Fig. 2).

Two samples from the Late Cretaceous Harebell Formation in northeastern Jackson Hole (Fig. 2) yielded Cretaceous ages of 73.1 ± 7.5 and 78.1 ± 9.5 Ma, respectively. The apatite crystals were detrital, and their individual grain ages were calculated (Table 2). The detrital ages from the lower part of the section had generally less scatter and clustered around 84 Ma. The upper sample's individual grain ages were more scattered, ranging from 55.1 to 98.8 Ma.

TABLE 2

Individual grain ages (Ma) and single population ages with 2σ errors of the Harebell Formation samples

SAMPLE I.D.	NUMBER OF (s) TRACKS COUNTED	NUMBER OF (i) TRACKS COUNTED	INDIVIDUAL AGE [Ma]	MEAN AGE ± 2-SIGMA ERROR [Ma]
HF-2 (upper elevation sample)	47	232	59.5	73.1± 7.5
	35	129	79.6	
	69	323	62.8	
	24	83	84.8	
	87	313	81.5	
	24	128	55.1	
	23	72	93.6	
	56	166	98.8	
	38	162	68.9	
	65	272	70.2	
HF-1 (lower elevation sample)	32	134	70.6	78.1± 9.5
	105	380	81.6	
	47	157	88.4	
	78	280	82.3	
	48	169	83.9	
	36	190	56.1	

4.2 Track-length measurements

The mean track lengths of the Rendezvous Peak sites (Fig. 4) decreased systematically with decreasing elevation and displayed a consistent breadth in the track-length distribution (± 1.5 μm). Similarly, the mean track lengths from Buck Mountain sites decreased with decreasing elevation. The track-length distributions, however, broadened considerably with decreasing elevation (Fig. 4).

The samples from Mount Moran contained fewer tracks than other samples and thus had fewer confined, horizontal tracks for track-length measurement. Nevertheless, the mean track lengths generally decreased with decreasing elevation (Fig. 4). The distributions of track lengths are consistent among all Mount Moran sites (± 2.0–2.4 μm), but are significantly larger than those distributions calculated for the more southerly sections.

Track-length distributions were also determined for the Gros Ventre site and one of the Harebell sites (Fig. 5). The track-length calibration sample (TR-14, Fig. 5) suggests that measurements were determined consistently. The mean track length for the Gros Ventre sample (GV-16) was 13.1 ± 1.9 μm, whereas that of the Harebell Formation sample (HF-2) was shorter (11.5 ± 2.2 μm) than most of the Teton samples.

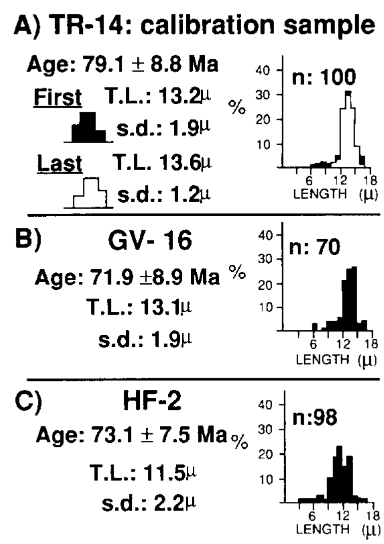

Fig. 5. (A) Age ($\pm 2\sigma$) and histogram of the track-length calibration sample (TR-14). First and last measurements compared in one graph. Mean track lengths (*T.L.*) and standard error (*s.d.*) recorded in μm. (B) Age ($\pm 2\sigma$) and histogram of the Gros Ventre sample. (C) Age ($\pm 2\sigma$) and histogram of the upper Harebell Formation sample. Medians of the μm measurements are 9.6 to 10.4 μm and have low standard errors. In the histograms, the y-axis is the percentage of tracks measured (rather than the number of measurements), because percentage measurements display more visible histograms for those samples with a low number of measurements.

5. Analysis and interpretation

5.1 Fission-track data

The Late Cretaceous to Oligocene fission-track ages reported for the Teton and Gros Ventre samples clearly do not represent the geologic ages of these rocks. These ages instead reflect a much later cooling through the apatite closure temperature. Many of the Precambrian and Cambrian rocks of the Teton Range and Gros Ventre Range were, therefore, cooled to temperatures below 105°C in the Late Cretaceous. As discussed below, many of the sampled rocks remained in the partial partial annealing zone, which would be expected to range from ~75–105°C for the fission-track ages determined here [20,21].

The samples from the two southernmost Teton sections display similar trends (Fig. 4), such that, with decreasing elevation, their fission-track ages and mean track lengths decrease. The mean track lengths (> 12.5 μm) and the relatively tight distribution of lengths ($\leqslant 1.5$ μm) for the upper two samples in the Rendezvous Peak and Buck Mountain sections indicate that they cooled through the apatite annealing isotherm and have resided above or near the top of the partial annealing zone since shortly after that time [20]. The lower samples, particularly in the Buck Mountain section, display broader track-length distributions indicating that they have spent considerable time within the partial annealing zone. It is important to note that, despite having resided within the partial annealing zone, the fission-track ages of the lower samples (TR-11, TR-15) are as little as 6 my younger than the non-annealed sample situated at the top of the section which is 1200 m higher than TR-11. This suggests that, despite partial annealing and track-length shortening, the ages of the lower samples are reasonably close approximations of the time of cooling below ~105°C. The Cretaceous fission-track ages of Rendezvous Peak and Buck Mountain samples indicate that the cooling recorded by their apatites was clearly not related to the Plio-Pleistocene uplift of the present-day Teton Range, but is instead an indicator of late Mesozoic cooling and related exhumation of the ancestral Tetons.

The Mount Moran section in the northern Tetons requires a somewhat different interpretation. In comparison to the two southern sections, the Mount Moran fission-track ages show a similar trend of decreasing age with decreasing elevation, but the range of ages, spanning from the latest Cretaceous at the top to latest Oligocene at the bottom (Fig. 4 and Table 1) is much greater than that encompassed by the other sections. Moreover, all except one sample (TR-32) display mean track lengths of < 12.5 μm and have broad track-length distributions (> 2 μm). This suggests that the entire section either has resided within the partial annealing zone for a considerable period since initial cooling in the Late Cretaceous or has been subjected to a post-Cretaceous heating event.

The 40.3 ± 4.9 Ma age of the Moose Pond FTD sample is intermediate between the Buck Mountain and Mount Moran dates at similar altitudes (Fig. 4). Although no track-length data are available for this sample, the coherent trend of ages among these three, low-altitude sites suggests that the Moose Pond sample also probably resided in the partial annealing zone for a significant interval of time.

The Gros Ventre sample, situated about 700 m below the Precambrian–Cambrian unconformity, yielded a fission-track age (71.9 ± 8.9 Ma) that is very similar to those of the Buck Mountain and Rendezvous Peak samples at comparable positions below the unconformity (Table 1). Although the mean track length of the Gros Ventre sample (Fig. 5B) is quite long (> 13 μm), the broad distribution of track lengths (± 1.9 μm) suggests that it, too, resided for some period within the partial annealing zone.

The mean fission-track ages of detrital apatites in the Harebell conglomerates are Late Cretaceous (Table 1). The array of individual ages at both sampling sites pass the χ^2 test [22] and indicate that a single population is present at each site. The mean track length (11.5 μm) and the breadth of the track-length distribution for these samples (Fig. 5C) indicate they have experienced some partial annealing, probably due to deep burial [20]. Because these apatite ages from the Harebell Formation are older than the depositional age, they can be interpreted as indicators of cooling and exhumation in the source area for the conglomerates. It is noteworthy that the lower Harebell sample yields an older age than the upper sample: a reversal of the age-vs.-elevation trend seen in the Teton sections. This is expected, however, because, unlike the Teton samples which were cooled in situ, the older detrital ages at the lower site are interpreted to represent the earliest cooled rocks that reached the erosion surface in the source area.

5.2 *Exhumation and crustal uplift rates*

Vertical displacement rates of the Teton Range in previous studies have been based upon the ages of offset marker beds. For 7 km of vertical basement separation over a period of ~ 9 my, Love [23] calculated an average rate of ~ 0.8 mm/yr. Vertical displacement across the Tetons of about 1500 m of the 2.05 Ma Huckleberry Ridge Tuff also yields an average offset rate of 0.8 mm/yr [6]. This observed offset represents a combination of footwall uplift and hanging-wall subsidence: ~ 5 km of the offset was accommodated through subsidence of the Jackson Hole basin east of the Teton Fault, and the remainder was accomplished through vertical uplift and westward tilting of the Teton Range itself.

Because many of the Teton samples have experienced partial annealing, direct calculations for all of the sections of either cooling or exhumation histories on the basis of the fission-track dates is not possible. However, well bracketed estimates can be made for the Buck Mountain section, and comparisons among the sections (Fig. 6) provide insights on their likely cooling histories. At Buck Mountain, the highest two samples appear to represent cooling ages with little or no subsequent annealing. The lower four samples display increasingly larger amounts of partial annealing, as evidenced by their systematically broadening track-length distributions (Fig. 4). The mean fission-track ages for these lower sites must be regarded as minimum ages, because annealing serves to decrease a sample's apparent age. If we

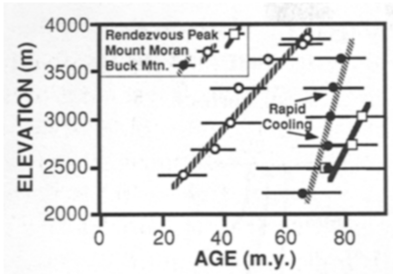

Fig. 6. Apatite fission-track age vs. elevation for the three vertical relief sections in the Teton Range. Assuming an unchanging geothermal gradient of 25°C/km, an interval of rapid cooling (50°C/10 my) characterizes the Buck Mountain section during the Late Cretaceous, during which time an exhumation/uplift rate of ~ 0.2 mm/yr prevailed. The lower slope of the Mount Moran data results from its smaller amount of documented Cretaceous cooling and its longer residence time in the zone of partial annealing.

assume that the fission-track ages represent times of cooling due to upward transit of the rock column through a stationary (with respect to its vertical separation from the erosional surface) 105°C isotherm which is identified with the lower limit of the partial annealing zone, a minimum bedrock uplift rate of 0.2 mm/yr between ~ 79 and 73 Ma can be determined for the Buck Mountain data. A rate of ~ 0.1 mm/yr is suggested for the upper two samples in the Rendezvous Peak section which appear to be unannealed. Although these rates are considerably less than the calculated late Cenozoic rates due to extensional offset, they are sufficiently high that they could not have been sustained during the entire Cenozoic; otherwise exhumation of a much greater magnitude than has been observed would have had to occur. Given the evidence for partial annealing of the lower elevation samples, it is likely that the exhumation recorded here only amounted to 1–2 km, such that the bases of these sections remained in the zone of partial annealing. Thus, these data provide evidence for a brief interval of cooling during the Late Cretaceous. Rather than resulting from a decrease in the geothermal gradient, this cooling is interpreted to result from relatively rapid Laramide crustal uplift and exhumation. The similarity of the age and track-length data from the Gros Ventre sample suggests that its Laramide cooling/exhumation history was very similar to that of the southern Teton Range.

5.3 Explanations of observed fission-track data

At least two explanations are possible to explain the fission-track data and the following observations: (1) Cretaceous fission-track ages predominate in the two southernmost sections, but not the northern one; (2) the age distribution along the range front suggests asymmetric cooling and exhumation; (3) the track-length data suggest that many of the samples have been subjected to temperatures sufficient to cause partial annealing; (4) the cooling/exhumation rates predicted by fission-track data do not match the rates calculated for late Cenozoic offsets of stratigraphic horizons; and (5) the Precambrian–Cambrian unconformity is significantly warped compared to its initial geometry. One possibility is that, following Laramide-aged cooling, subsequent heating of the range from outside sources caused partial annealing of the entire northern part of the Tetons, as well as the lower part of the southern Tetons. A second possibility is that the southern and central parts of the range were uplifted and cooled prior to the northern Tetons, causing doming of the Precambrian–Cambrian unconformity, and that the entire Mount Moran section, as well as much of the southern sections, remained in the partial annealing zone until a more recent interval of uplift.

Thermal modeling

To test the possibility that thermal perturbations affected the northern end and the lower parts of the southern and central Tetons, heat-flow modeling was applied to two of the most likely heat sources near the Tetons: the magma body below the Yellowstone volcanic field (Fig. 1) and a volcanic source for the Miocene volcaniclastic Colter Formation (Fig. 2).

The magma body beneath the Yellowstone volcanic field was active by ~ 4 Ma at the Island Park caldera [24], the western caldera in Fig. 1. A one-dimensional, infinite planar model that was designed to calculate temperature effects was applied to the magma body. Following the intrusive sheet model of Jaeger [25], the basic heat-conduction equation was numerically evaluated as follows [26]:

$$\rho \cdot c \cdot \frac{\partial T}{\partial t} = K \cdot \frac{\partial^2 T}{\partial x^2} \qquad (1)$$

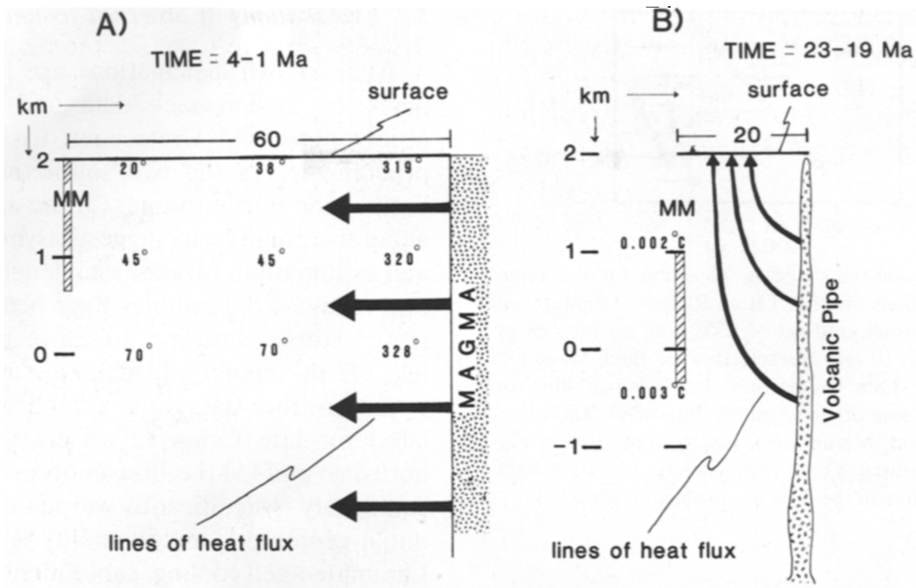

Fig. 7. (A) Schematic diagram of effects of a one-dimensional heat-conduction model. Yellowstone magma body is the heat source; *MM* represents the Mount Moran rock column that was potentially heated. Arrows represent direction of heat flux. Calculated temperatures are depicted at various depths. The model ignores any heat loss to surface and thus overestimates any potential thermal effects on the Mount Moran rock column. (B) Schematic diagram of a volcanic vent as a linear heat source and Mount Moran (*MM*) as the potentially heated rock column. Arrows represent direction of heat flux. Only small fractions of a degree of additional heating are estimated for areas 20 km from the vent.

where ρ is density (g/cm^2), c is specific heat (J/g · K), K is thermal conductivity (J/cm · s · K), T is temperature (K), x is distance between heat source and potentially heated rock (cm), and t is time (s). For simplicity, effects due to convection were neglected, heat flux was maximized between source (the magma body) and the northern Tetons, and heat loss at the surface was ignored (see heat flux arrows in Fig. 7A).

The solution to eq. (1) is the tabulated error function erf λ, where:

$$\operatorname{erf} \lambda = \frac{2}{\sqrt{\pi}} \int_0^{\lambda} e^{-x^2} \partial x \tag{2}$$

Using the calculated λ value for the appropriate rock and magma type, the temperature of potentially heated rocks can be calculated [25]. At distance x from the heat source and at time t of activity, this equation is:

$$T_s = \frac{T_1}{1 + \operatorname{erf} \lambda} \cdot \left(1 + \operatorname{erf} \frac{x}{2\sqrt{(k \cdot t)}}\right) \tag{3}$$

where T_s is temperature of potentially heated rocks (°C), T_1 is temperature of magma at specified depths (°C), erf λ is error function of eq. (2), x is distance (cm), t is time (s), and k is thermal diffusivity $= K/\rho \cdot c$ (cm^2/s). This study uses a λ value [25] of 800°C for rhyolitic magma [27].

Subsurface temperatures (T_s) were calculated for varying distances (x) and time (t) as shown in Fig. 7A. The modelled calculations do not indicate any significant heating effects at Mount Moran for the maximum time and minimum distance that are geologically likely.

The second heat source tested for possible heating of the northern Teton Range was the volcanic source body of the Colter Formation, whose vent was possibly located under northern Jackson Lake within 20 km of Mount Moran. Barnosky [13] estimated that numerous eruptions would have occurred from this andesitic source between 24 and 18 Ma. This source would not have had an immense, shallow magma body such as the one under Yellowstone, but rather a narrow, linear pipe extending from a deep magma chamber to the surface.

An appropriate model for linear heat conduction in the earth is a sum of instantaneous point sources with corresponding image sources to constrain the earth's surface at constant temperature [28]. Based on Carslaw and Jaeger's equation [28] that solves for temperature resulting from the summation of point sources, a simplified equation is used to solve for temperature:

$$T = \frac{Q}{8(\pi kt)^{\frac{3}{2}}}\left[\left(e - R_1^2/4kt\right) - \left(e - R_2^2/4kt\right)\right] \tag{4}$$

where Q is heat flux (°C · cm^3), R_1 refers to a radial distance between source and potentially heated rock (km), and R_2 is the radial distance between the image source and the rock (km); the other variables follow as above in eqs. (1) and (3). The melting temperature of andesitic magma was estimated at 950°C [27]. The earth's surface is assumed to be 0°C at the surface, and heat loss through the surface occurred as shown by the arrows in Fig. 7B. Temperature perturbations were determined at specified times and distances from the source, and then were summed for each increment of source depth and time with respect to R_1 and R_2, providing one temperature for the rock in question. The results (Fig. 7B) indicate that, for a probable depth of 1 to 2 km below an assumed mean surface at 24 to 18 Ma, the Mount Moran rocks would have been perturbed < 1°C at the top and bottom of the rock column from the modeled Colter volcanic source.

The modeling results indicate that neither of these heat sources provides a viable mechanism for partial annealing of the Teton apatites. Consequently, the fission-track ages and track-length distributions must be interpreted in terms of a cooling and exhumation history.

Exhumation / crustal uplift history

The rocks constituting the Teton Range clearly experienced doming at some time, as shown by the geometry of the Precambrian–Cambrian unconformity which crops out at the north and south ends of the range near the valley floor, but which has been eroded from above the highest peaks along the eastern escarpment in the center of the range (Figs. 3 and 4). Isochrons representing similar fission-track ages, as well as contours of equal track length and track-length distribution, illustrate the asymmetry of deformation along the eastern escarpment (Fig. 8). The rise toward the north of each of these indicators suggests that the Mount Moran section resided longer in the partial annealing zone and was

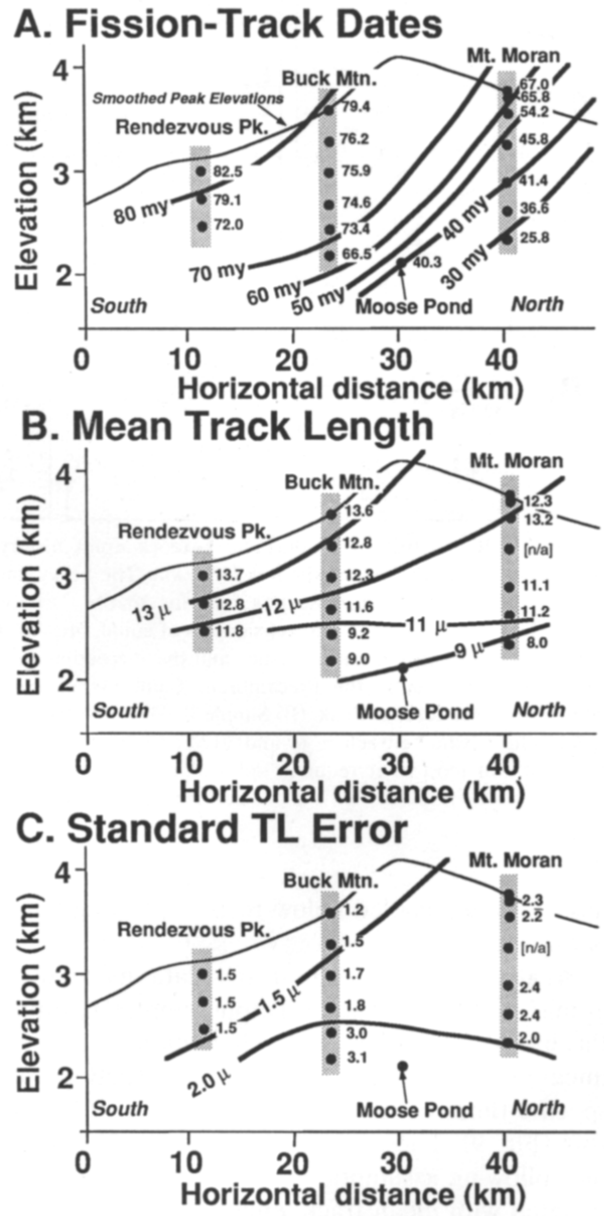

Fig. 8. (A) Isochrons of fission-track ages projected on to a N–S cross-section of the Teton Range. The light line is the smoothed peak elevations; heavy lines are isochrons. The fission-track ages (my) of the samples at their elevations serve as calibration points. Vertical exaggeration is ×3.3. (B) Lines of equal mean track length generally rise to the north and provide evidence that the more northerly sections and the lower parts of each section spent more time in the partial annealing zone. (C) Spatial array of the standard error on the track-length distributions indicates that many of the sites have experienced partial annealing.

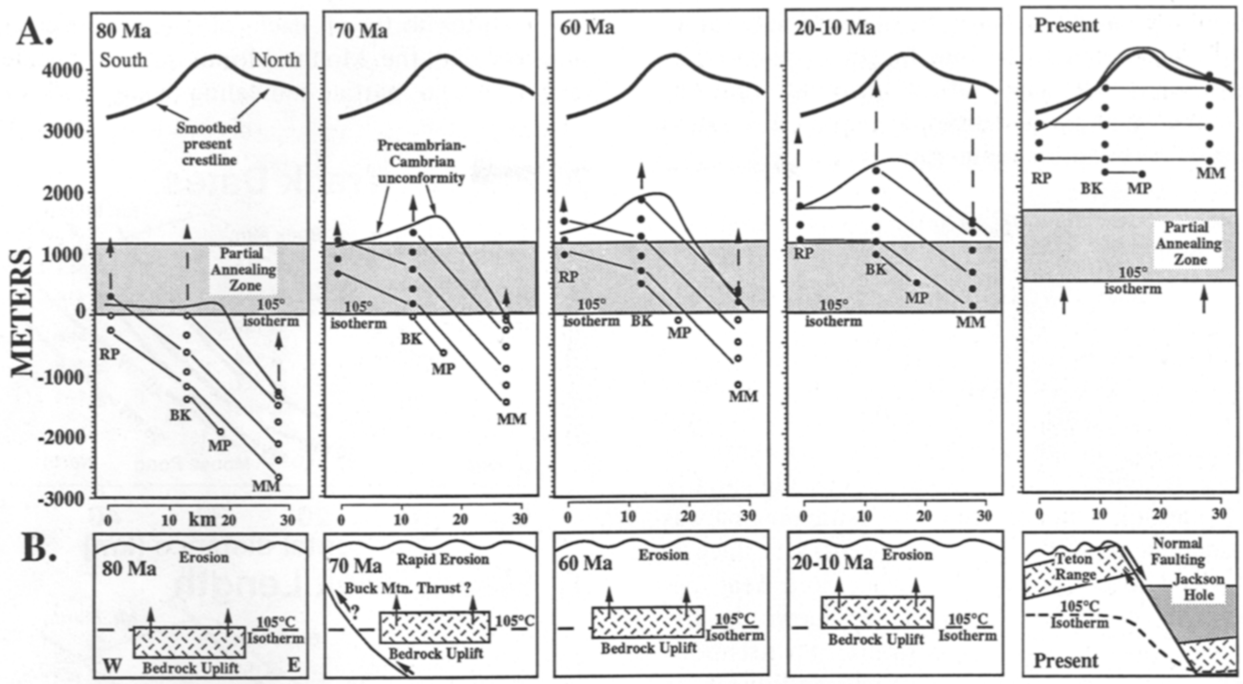

Fig. 9. (A) Reconstructed cooling and bedrock uplift history of equal-elevation samples through time projected along a N–S cross-section. Geothermal gradient = 25°C/km. The heavy line in each diagram is the present-day mean peak elevations. Shaded box represents the partial annealing zone for apatite. ○ = samples at temperatures higher than 105°C; ● = samples cooler than 105°C. The thin, solid lines connect samples of equal, present-day elevation. Vertical, dashed arrows represent the amount of uplift that occurs between a given time slice and the succeeding one. The progression of bedrock uplift can be tracked by following the changing orientation of the Precambrian–Cambrian unconformity. *BK* = Buck Mountain; *MM* = Mount Moran; *MP* = Moose Pond; *RP* = Rendezvous Peak. (B) Simple E–W cross-section through the Teton Range in the vicinity of Buck Mountain. The most rapid uplift occurs between ~ 80 and 70 Ma. Some of this may be locally attributable to motion of the Buck Mountain Thrust (70 Ma?[12]), but most of it requires uplift along deeper seated, more regional structures. Rapid late Cenozoic extension strongly perturbs the annealing isotherm across the normal fault.

more recently cooled below these annealing temperatures.

Analysis of the fission-track data using diagrams of equal-elevation Teton samples permits the history of cooling and exhumation to be delineated through a series of reconstructions at specific times in the Late Cretaceous and Cenozoic (Fig. 9). These reconstructions are based on the following assumptions: fission-track dates associated with mean track lengths > 12.5 μm and track-length distributions of < 1.5 μm represent times of cooling below 105°C and removal from the zone of partial annealing shortly thereafter; those samples with shorter mean track lengths and larger uncertainties in the track-length distribution represent minimum ages for cooling below 105°C and have spent considerable time in the partial annealing zone, such that the residence time is approximately proportional to the deviation from the track-length values cited above; the 105° annealing isotherm was regionally subhorizontal in the past; the geothermal gradient was assumed constant at ~ 25°C/km and the surface temperature was assumed to be 10°C; a partial annealing zone existed between the 75°C and 105°C isotherms; cooling was due to upward transport of bedrock toward the erosional surface, rather than due to lowering of the local geothermal gradient (thus, the rate of erosional lowering of the landscape (exhumation) balances the rate of bedrock uplift); dips between sections are defined on the basis of coeval non-annealed dates in each section; and both the presently observable thicknesses of the sections and the vertical position of the unconformity with respect to each section has not changed through time. The general configuration of the unconformity through time can also be specified with respect to four tie points: the unconformity lies just below the topmost sample sites of the Rendezvous Peak and Mount Moran sections, it lies more than 200 m above the top of the Buck Mountain section, and it is located more than 2 km above the Moose Pond site.

Given the above assumptions, the reconstructions (Fig. 9) indicate that cooling was underway by 80 Ma as the southern sections crossed or approached the 105°C isotherm. At this time, there was a distinctive, two-part dip of the unconformity: its northern portion sloped steeply down from above the Moose Pond site to the top of the Mount Moran section, whereas the southern half was essentially horizontal. It is not possible to specify when cooling and exhumation initiated, because the tops of each of the studied sections have been eroded. Nonetheless, given the evidence for differential cooling between the various sections (Fig. 6) and the folding of the unconformity, it appears that uplift was likely to have commenced somewhat earlier in the southern Tetons in order to deform the Precambrian–Cambrian unconformity which was initially created as a subhorizontal surface. It is possible, however, that this deformation occurred long before the Late Cretaceous events described here.

Because some or all dates are available for all three relief sections at ~ 70 Ma, the most reliable geometry can be reconstructed at this time. Whereas the top of the Mount Moran section was near the 105°C isotherm, ~ 1 km of additional bedrock uplift of the Buck Mountain section at rates as high as 0.2 mm/yr had occurred by this time, such that the top part of the section was above the zone of partial annealing. This uplift was sufficiently more rapid than that of the Rendezvous Peak section that the unconformity was also folded toward the south between them (Fig. 9A). Some of the differential offset may be been accommodated by Laramide shortening (Fig. 9B) on the Buck Mountain Thrust [11]. Range-scale cooling, however, can not be attributed to movement on this fault, due to its local nature. Instead a deeper seated, more regional structure must have been active at this time.

By 60 Ma, only the basal parts of the Rendezvous Peak and Buck Mountain sections were present within the partial annealing zone, whereas the Mount Moran section was still entirely located within or below this zone. Given the fission-track ages and the rock columns encompassed by each section, it is important to note that, at that time, the unconformity still dipped steeply to the north from the Buck Mountain section and dipped more gently to the south. In this reconstructed deformational sequence, this interval is approximately the end of relatively rapid bedrock uplift. Some slower uplift due to isostatic adjustments in response to erosional unloading or further tectonically induced deformation probably occurred in the succeeding 40 my, but the net uplift was slower and was likely to be limited to 0.3–1.0 km.

The timing and general amount of the final stage (Miocene to Pleistocene) of uplift was determined on the basis of the previously discussed stratigraphic data [6,9,23] related to the offset of marker horizons during extensional faulting. It is interesting to note that, based upon the reconstructed curvature of the unconformity in the previous steps (80–60 Ma; Fig. 8), large-scale differential uplift occurred during this interval. In the northern part of the range, ~ 2.5 km of footwall uplift occurred, whereas only 1 km occurred in the southern part of the range. This differential uplift was responsible for rotating the unconformity into its present orientation. Overall, between 80 Ma and present, the unconformity was uplifted ~ 3 km in the south and 5 km in the north, yielding a net rotation of about 3° to the south.

6. Summary and conclusions

Fission-track dating and track-length studies of apatites reveal significant contrasts between the northern and southern parts of the Teton Range. Older ages, longer mean track lengths, and smaller variance in track-length distributions in the southern Tetons (Rendezvous Peak and Buck Mountain sections) indicate that those samples experienced a pulse of Late Cretaceous cooling. The upper parts of these sections have been situated above the apatite partial annealing zone since that time, whereas the lower parts display the effects of partial annealing. The observations that the fission-track ages in the northern Tetons are younger and that the track-length data here provide abundant evidence of partial annealing indicate that the presently preserved bedrock in the Mount Moran area clearly cooled later and resided in the partial annealing zone longer than did the southern Teton sections. Heat-flow modeling of two reasonable thermal sources (the Yellowstone magma chamber and the Colter volcanics) indicates that the observed annealing is very unlikely to have resulted from heating due to igneous activity. Instead, if subhorizontal isotherms are assumed, the configuration of ages and track lengths dictates that the Precambrian–Cambrian unconformity was significantly folded by the end of this Cretaceous deformation, such that it dipped northward and displayed ~ 1.5 km of relief along the range front.

Based on the assumptions that the local geothermal gradient was not significantly decreasing at this time and that the region had not been subjected to a recent heating episode, the observed cooling can be interpreted as related to exhumation that occurred in response to bedrock uplift. If it is also assumed that rates of exhumation and bedrock uplift were equal, then the cooling histories represent ~ 1.5–2 km of uplift at rates of 0.1–0.2 mm/yr during the Late Cretaceous. If the bedrock uplift rates exceeded exhumation rates and if there was also an upward perturbation of the local isotherms due to uplift, then the magnitude of uplift may have been greater than this.

These data from the southern Tetons and those from the Gros Ventre Range are similar to the apatite fission-track data from parts of the Wind River Range (Fig. 1), where limited, Late Cretaceous uplift at rates of 0.2–0.3 mm/yr also occurred [29]. Thus, the Laramide deformation that has been documented in the Wind River Range can be extended to the Teton Range. Although motion along previously defined, large-scale, basement-involved reverse faults can be invoked to explain the Wind River uplift, no similar faults have been well documented for the Teton area. The nature of the cooling history described here for the Teton region, however, demands that deep-seated Laramide structures were active at this time. Deformation of the Phanerozoic cover, unless it involved extensive detachment and extension, could not explain the observed basement cooling or the folding of the unconformity. Weakly constrained reconstructions of Laramide motion on the Buck Mountain fault suggest that ~ 1 km of shortening may have occurred here [11]. In theory this could explain the observed cooling at the Buck Mountain section. No comparable fault can be invoked, however, for the Mount Moran or Rendezvous Peak sections. Motion on the deeper seated, west-vergent Cache Creek fault may be more likely to have caused the observed cooling. Regardless of the precise mechanism of shortening, the cooling data discussed here require considerable Laramide motion along basement-involved structures within the Teton region, as well as in the Wind River Range.

Zircons from the Tetons, like those from the Wind River Range [29], are totally or partially metamict. This indicates that these rocks have not been heated above the zircon annealing temperature for hundreds of millions of years, and also suggests that neither the Teton Range nor the Wind River Range has experienced more than 9 km of uplift during the last half of the Phanerozoic. Late Cenozoic extension has offset the basement by ~ 7 km, but the majority of this offset is accommodated through hanging-wall subsidence (5 km). Although only ~ 2 km has expressed itself as footwall uplift, this uplift has given rise to the present-day edifice of the Teton Range, and it represents the most recent stage of a prolonged deformational history that began at least as early as the Late Cretaceous.

Acknowledgements

Acknowledgment is made for the generous support of the donors to the Petroleum Research Fund, administered by the American Chemical Society (ACS-PRF 15324-G2). Additional support for this research was provided by the University of Southern California Faculty Research and Innovation Fund, the Department of Geological Sciences at USC, the Geological Society of America, and AAPG. Irradiations were performed in the TRIGA reactors at USGS (Denver, CO) and at Oregon State University (Corvallis, OR). Apatite track lengths were measured and analyzed at the USGS FTD lab in Denver with the much appreciated guidance of C. Naeser. Very helpful comments on an earlier version of this paper by J. Steidtmann, C. Naeser, and an anonymous reviewer have served to improve this paper greatly and are appreciated by the authors.

References

1 A.J.W. Gleadow and P.G. Fitzgerald, Uplift history and structure of the Transantarctic Mountains: new evidence from fission-track dating of basement apatites in the Dry Valleys area, southern Victoria Land, Earth Planet. Sci. Lett. 82, 1–14, 1987.

2 C.W. Naeser, B. Bryant, M.D. Crittenden, Jr. and M.L. Sorensen, Fission-track ages of apatite in the Wasatch Mountains, Utah: an uplift study, Geol. Soc. Am. Mem. 157, 29–36, 1983.

3 P.K. Zeitler, R. Tahirkheli, C.W. Naeser and N.M. Johnson, Unroofing history of a suture zone in the Himalaya of Pakistan by means of fission-track annealing ages, Earth Planet. Sci. Lett. 57, 227–240, 1982.

4 J.C. Reed, Jr. and R.E. Zartman, Geochronology of Precambrian rocks of the Teton Range, Wyoming, Geol. Soc. Am. Bull. 84, 561–582, 1973.

5 W.G. Brown, Basement-involved tectonics: foreland areas, Am. Assoc. Pet. Geol. Cont. Educ. Course Notes 26, 1–92, 1984.

6 J.D. Love, Summary of upper Cretaceous and Cenozoic stratigraphy, and of tectonic and glacial events in Jackson Hole, northwest Wyoming, Wyo. Geol. Assoc. Guidebook, 29th Annu. Field Conf., pp. 585–593, 1977.

7 R.K. Dokka, M.J. Mahaffie and A.W. Snoke, Thermochronologic evidence of major tectonic denudation associated with detachment faulting, northern Ruby Mountains: East Humboldt Range, Nevada, Tectonics 5, 995–1006, 1986.

8 D.S. Miller and S. Lakatos, Uplift rate of Adirondack anorthosite measured by fission-track analysis of apatite, Geology 11, 284–286, 1983.

9 J.D. Love, J.C. Reed, Jr., R.L. Christiansen and J.R. Stacy, Geologic block diagram and tectonic history of the Teton Range, Wyoming–Idaho, US Geol. Surv. Misc. Geol. Invest. Map I-730, 1973.

10 J.C. Behrendt, B.L. Tibbetts, W.E. Bonini and P.M. Lavin, A geophysical study in Grand Teton National Park and vicinity, Teton County, Wyoming, US Geol. Surv. Prof. Pap. 516-E, 23 pp, 1968.

11 J.G. Schmitt, Origin of Late Cretaceous to Early Tertiary quartzite conglomerates in northwestern Wyoming, Wyo. Geol. Assoc. Guidebook, 38th Ann. Field Conf., pp. 217–224, 1987.

12 D.J. Smith, Structural Geology and History of the Buck Mountain Fault and Adjacent Intra-range Faults, Teton Range, Wyoming, 143 pp, MSc thesis, Montana State Univ., Bozeman, 1991 (Unpubl.).

13 A.D. Barnosky, The Colter Formation: evidence for Miocene volcanism in Jackson Hole, Teton County, Wyoming, Wyo. Geol. Assoc. Earth Sci. Bull. 16, 50–101, 1984.

14 C.W. Naeser, Fission-track dating, US Geol. Surv. Open-File Rep. 76-190, 1978.

15 A.J.W. Gleadow, Fission-track Dating Methods II – A Manual of Principles and Techniques: Workshop on Fission-track Analysis: Principles and Applications, 49 pp., James Cook Univ., 1984.

16 V.E. McGee, N.M. Johnson, and C.W. Naeser, Simulated fissioning of uranium and testing of the fission-track dating method, Nucl. Tracks 10, 365–379, 1985.

17 P.F. Green, I.R. Duddy, G.M. Laslett, K.A. Hegarty, A.J.W. Gleadow and J.F. Lovering, Thermal annealing of fission tracks in apatite 4. Quantitative modelling techniques and extension to geological timescales, Chem. Geol. (Isot. Geosci. Sect.) 79, 155–182, 1989.

18 A.J.W. Gleadow, I.R. Duddy, P.F. Green and J.F. Lovering, Confined fission-track lengths in apatite: a diagnostic tool for thermal history analysis, Contrib. Mineral. Petrol. 94, 405–415, 1986.

19 G.M. Laslett, A.J.W. Gleadow and I.R. Duddy, The relationship between fission-track length and density in apatite, Nucl. Tracks 9, 29–38, 1984.

20 P.F. Green, I.R. Duddy, A.J.W. Gleadow, and J.F. Lovering, Apatite fission-track analysis as a paleotemperature indicator for hydrocarbon exploration, in: Thermal History of Sedimentary Basins, N.D. Naeser and T. McCulloh, eds., pp. 181–196, Springer, New York, NY, 1989.

21 N.D. Naeser, C.W. Naeser, and T.H. McCulloh, The application of fission-track dating to the depositional and thermal history of rocks in sedimentary basins, in: Thermal History of Sedimentary Basins, N.D. Naeser and T. McCulloh, eds., pp. 157–180, Springer, New York, NY, 1989.

22 R. Galbraith, On statistical methods for fission track counts, Math. Geol. 13, 471–488, 1981.

23 J.D. Love, Teton mountain front, Wyoming, Geol. Soc. Am. Centen. Field Guide, Rocky Mtn. Sect., pp. 173–178, 1987.

24 R.L. Armstrong, W.P. Leeman and G.E. Malde, K–Ar dating, Quaternary and Neogene volcanic rocks of the Snake River Plain, Idaho, Am. J. Sci. 275, 225–251, 1975.

25 J.C. Jaeger, The temperature in the neighborhood of a cooling intrusive sheet, Am. J. Sci. 255, 306–318, 1957.

26 D.L. Turcotte and G. Schubert, Geodynamics: Applications of Continuum Physics to Geological Problems, 450 pp., Wiley, New York, NY, 1982.

27 W. Hildreth, Gradients in silicic magma chambers: implications for lithospheric magmatism, J. Geophys. Res. 86, 10,153–10,192, 1981.

28 H.S. Carslaw and J.C. Jaeger, Conduction of Heat in Solids, 510 pp., Oxford Univ. Press, Oxford, 1959.

29 P.F. Cerveny and J.R. Steidtmann, Fission-track thermochronology of the Wind River Range: evidence for differential uplift of the Laramide foreland, Geol. Soc. Am. Abstr. Prog. 21, 266, 1989.